**Article:**
Zhao, M, Bilton, M, Brown, AP et al. (2014) Durability of CaO–$CaZrO_3$ Sorbents for High-Temperature $CO_2$ Capture Prepared by a Wet Chemical Method. Energy and Fuels, 28 (2). pp. 1275-1283. ISSN: 0887-0624

https://doi.org/10.1021/ef4020845

# Durability of $CaO$-$CaZrO_3$ sorbents for high-temperature $CO_2$ capture prepared by a wet chemical method

*Ming Zhao*[*,†], *Matthew Bilton*[†], *Andy P Brown*[†], *Adrian M Cunliffe*[‡], *Emiliana Dvininov*[§], *Valerie Dupont*[‡], *Tim P Comyn*[†], *Steven J Milne*[†]

[†] Institute for Materials Research, SPEME, University of Leeds, Leeds LS2 9JT, United Kingdom

[‡] Energy Research Institute, SPEME, University of Leeds, Leeds LS2 9JT, United Kingdom

[§] MEL Chemicals, Swinton, Manchester M27 8LS, United Kingdom

## ABSTRACT

Powders of CaO sorbent modified with $CaZrO_3$ have been synthesized by a wet-chemical route. For carbonation and calcination conditions relevant to sorbent enhanced steam reforming applications, a powder of composition 10 wt% $CaZrO_3$: 90 wt% CaO showed an initial rise in $CO_2$ uptake capacity in the first 10 carbonation–decarbonation cycles, increasing from 0.31g-$CO_2$/ g-sorbent in cycle 1 to 0.37 g-$CO_2$/ g-sorbent in cycle 10 and stabilizing at this value for the remainder of the 30 cycles tested: carbonation at 650 ℃ in 15% $CO_2$; calcination at 800 ℃ in air. Under more severe conditions of calcination at 950 ℃ in 100% $CO_2$ following carbonation at 650 ℃ in 100 % $CO_2$, the best overall performance

was for a sorbent with 30 wt% $CaZrO_3$: 70 wt% CaO (the highest Zr ratio studied), with an initial uptake of 0.36 g-$CO_2$/g-sorbent decreasing to 0.31 g-$CO_2$/g-sorbent at the 30$^{th}$ cycle. Electron microscopy revealed $CaZrO_3$ was present in the form of ≤ 0.5 μm cuboid and 20-80 nm particles dispersed within a porous matrix of $CaO/CaCO_3$; the nanoparticles are considered to be the principal reason for promoting multicycle durability.

## Introduction

Powder sorbents for capturing $CO_2$ at high temperatures find applications in a number of areas. Calcium oxide is of interest for post-combustion capture (PCC) from fossil-fuel fired power plants and other single-point industrial emitters [1]. Calcium-looping PCC, based on the reversible reaction $CaO+CO_2 \leftrightarrows CaCO_3$, can be implemented using two parallel fluidized beds operated as a carbonator and a regenerative calciner, typically at ≥ 650 $^oC$ in ~ 15% $CO_2$ and ≥ 950 $^oC$ in ~100% $CO_2$ respectively [2]. Another area of application of CaO powder sorbents lies in steam reforming for the production of $H_2$, whereby removal of the $CO_2$ co-product shifts the reaction equilibrium in favor of greater $H_2$ yields and purity [3]. Conditions for carbonation are comparable to those of PCC, i.e. ~600 °C in ~15 % $CO_2$ however, when oxygen looping is employed in sorption enhanced steam reforming (SESR) overall enthalpy is reduced by the exchange of oxygen through a metal catalyst and the regeneration of the sorbent is carried out in air at temperatures ≥ 800 °C [4]. Hence sorbent regeneration conditions for SESR are considerably less severe than for PCC, but nevertheless unmodified CaO shows serious loss of $CO_2$ capacity after repeated calcination cycles leading to lower $H_2$ yields [5, 6]. Thus, there is an economic need to develop high reactivity CaO-based sorbents that maintain performance between 0.3 to 0.78 g-$CO_2$/g-sorbent over multiple $CO_2$ capture cycles for SESR applications [7, 8].

Improvements to CaO-sorbents have been achieved by the addition of second-phase refractory 'spacer' particles to inhibit densification of the CaO particle matrix [6, 9-20]. It should be noted that refractory additives to CaO, inhibit densification not merely due to physical separation of the sorbent particles, but also due to differential thermal expansion effects and differential sintering rates of the two components resulting in stresses that inhibit densification [21]. **Table 1** shows examples of the multi-cycle performance of modified CaO sorbent powders under various looping conditions, which can be broadly categorized as 'mild' calcination (≤800 $^{o}$C, requiring very low $CO_2$ partial pressures for decarbonation) and 'severe' calcination conditions (>900 $^{o}$C in the presence of high partial pressures of $CO_2$). Calcination conditions have a major effect on durability [8], with increased calcination temperatures and dwell times giving increased densification, lower porosity and lower $CO_2$ uptake within the timescale of each cycle (≥ 5 cycles), however the preceding carbonation conditions also affect the degree of densification during calcination. Carbonate decomposition initially produces a porous structure: the more extensive the carbonation reaction the greater the degree of porosity generated on initial decarbonation which can result in less densification at the completion of the calcination cycle. Near full carbonation (100 % conversion ratio of CaO) is achievable within each cycle by using relatively high temperatures, prolonged dwell times and $CO_2$ rich atmospheres. Therefore, carbonation and decarbonation (calcination) conditions should both be considered when comparing durability performance data from different laboratories (Table 1). The multicycle reactivity of CaO is also affected by the steam content of the feed stream; steam treatments, or other forms of hydration, have been shown to improve performance due to structural changes associated with $CaO \leftrightarrow Ca(OH)_2$ interconversion [22-24].

There has been considerable focus on the $CaO:Al_2O_3$ sorbent system because the *in-situ* formation of $Ca_{12}Al_{14}O_{33}$ particles hinders densification and sintering of the CaO phase

during calcination [9-13]. A number of other 'spacer' particle additives are also reported, for example: CaO:$CaTiO_3$ [14], CaO:MgO [15], CaO:$Y_2O_3$ [16] and CaO:$SiO_2$ [6] The performance of these materials is also summarized in Table 1.

Here we report on the development of $ZrO_2$ as a potential stabilizer for CaO sorbents because the two components react at elevated temperatures to form a thermodynamically stable binary mixture of CaO and $CaZrO_3$ [17-20]. Lu et al. employed a flame spray pyrolysis (FSP) technique to prepare zirconia modified CaO sorbents [17]. They identified an optimum molar ratio $n_{Zr}$:$n_{Ca}$ = 3:10 that retained a stable 64% molar conversion ratio (equal to a net $CO_2$ capture capacity of 0.30 g-$CO_2$/g-sorbent) after 23 cycles for calcination at 700 °C in He (carbonation at 700 °C in 30 % $CO_2$ for 30 min). For a more severe calcination temperature of 950 °C, a greater change in uptake was observed, with the molar conversion ratio falling to 50 % after 23 cycles [17]. Wet chemical synthesis of the same powder composition, $n_{Zr}$:$n_{Ca}$=3:10, using co-precipitation from calcium nitrate and zirconyl nitrate solutions resulted in inferior performance compared to the FSP powder such that the conversion ratio decreased from ~60 to 30 % after 23 cycles. The difference was attributed to the lower surface area of the wet chemical powder [17]. The same group later reported $n_{Zr}$:$n_{Ca}$=5:10 powders prepared by the same method but containing 56 wt% $CaZrO_3$ gave optimum performance [18]. For very mild calcination conditions at 700 °C for 10 min in He (after carbonation in 100 % $CO_2$) a conversion ratio of ~60 % was retained after >100 cycles, equating to ~0.23 g-$CO_2$/g-sorbent. Increasing the calcination temperature to 950 °C (in 30% $CO_2$ after carbonation at 850 °C in 100 % $CO_2$) showed a drop in performance relative to mild calcination, but nevertheless a conversion ratio of ~55% was retained after 100 cycles [18]. Radfarnia and Iliuta produced Zr-modified CaO sorbents using a surfactant templated ultrasound synthesis method [19]. The best powders, $n_{Zr}$:$n_{Ca}$=3.03:10 exhibited a drop in molar conversion ratio from ~32 % in cycle 1 to ~24 % in cycle 15. This corresponded to a $CO_2$

uptake of 0.19 g-$CO_2$/g-sorbent in cycle 1, and 0.14 g-$CO_2$/g-sorbent in cycle 15, for mild calcination at 750 °C in Ar following carbonation at 600 °C in 100 % $CO_2$ [19]. Most recently, Broda and Muller have reported a sol-gel method using zirconium propoxide as the gelling agent [20]. Their best $ZrO_2$ stablised CaO sorbents were obtained using $Ca(OH)_2$ as a precursor for CaO and a gelling time of 2 h. Under relatively severe conditions (carbonation in 20% $CO_2$ at 650 $^oC$ for 20 min, calcination in 100% $CO_2$ at 900 $^oC$ for 10 min), the sorbents with the highest mass fraction of CaO (80wt%CaO20wt%$ZrO_2$ and 90wt%CaO10wt%$ZrO_2$) showed $CO_2$ uptakes at cycle 10 of 0.31 and 0.36 g-$CO_2$/g-sorbent, respectively. In contrast, the sorbents with a higher-Zr mass fraction had lower initial uptake but were more stable over multiple cycles, for example the uptake for 64wt%CaO36wt%$ZrO_2$ decayed from an initial value of 0.33 to 0.21 g-$CO_2$/g-sorbent after 10 cycles [20].

The present work concerns an alternative wet chemical powder synthesis method for $CaZrO_3$/CaO sorbent powders, tested over 30 carbonation-decarbonation cycles. We show that the overall performance is superior to other Zr- modified CaO sorbents produced by solution-precipitation routes: near-stable multicycle $CO_2$ capture performance, after an initial rise, is demonstrated for mild conditions relevant to SESR involving carbonation at 650 °C in 15 % $CO_2$ and calcination in air at 800 °C. The sorbents are also evaluated under severe conditions relevant to PCC: here, the capture capacity declines by <15% of the original value of 0.36 g-$CO_2$/ g-sorbent by cycle 30. Scanning and transmission electron microscopy utilizing selected area electron diffraction, atomic lattice imaging and energy dispersive X-ray spectroscopy with elemental mapping are used to investigate reasons for the favorable performance of the powders.

**Table 1.** Summary of previous reports on spacer-CaO adsorbents

| Authors [ref.] | Sorbents (mass ratio) | Carbonation | | | Calcination | | | Number of cycles | Net $CO_2$ uptake (g-$CO_2$/g-sorbent) | |
|---|---|---|---|---|---|---|---|---|---|---|
| | | Atmosphere | $T$ ($^o$C) | $t$ (min) | Atmosphere | $T$ ($^o$C) | $t$ (min) | | initial | final |
| Li et al. [9] | 75%CaO25%$Ca_{12}Al_{14}O_{33}$ | 14% $CO_2$ | 690 | 30 | 100% $N_2$ | 850 | 10 | 13 | 0.40 | 0.45 |
| | | 14% $CO_2$ | 690 | 30 | 20% $CO_2$ | 950 | 10 | 13 | 0.42 | 0.33 |
| Martavaltzi and Lemonidou [10] | 85%CaO15%$Ca_{12}Al_{14}O_{33}$ | 15% $CO_2$ | 690 | 30 | 15% $CO_2$ | 850 | 5 | 45 | 0.45 | 0.36 |
| | 75%CaO25%$Ca_{12}Al_{14}O_{33}$ | 15% $CO_2$ | 690 | 30 | 15% $CO_2$ | 850 | 5 | 45 | 0.35 | 0.3 |
| Koirala et al. [11] | $n_{Al}$:$n_{Ca}$=3:10 | 30% $CO_2$ | 700 | 10 | 30% $CO_2$ | 700 | 10 | 100 | 0.39 | 0.39 |
| Broda and Muller [12] | $n_{Al}$:$n_{Ca}$=1:9 | 55% $CO_2$ | 750 | 20 | 100% $N_2$ | 750 | 20 | 30 | 0.52 | 0.55 |
| | | 100% $CO_2$ | 850 | 10 | 30% $CO_2$ | 950 | 10 | 100 | 0.36 | 0.25 |
| Yu and Chen [13] | 76%CaO10%$Al_2O_3$14%$TiO_2$ | 100% $CO_2$ | 750 | 60 | 100% $N_2$ | 750 | 30 | 15 | 0.40 | 0.36 |
| Wu and Zhu [14] | 90%CaO10%$TiO_2$ | 20% $CO_2$ | 600 | 10 | 100% $N_2$ | 750 | 10 | 10 | 0.20 | 0.24 |
| Li et al. [15] | 58%CaO42%MgO | 100% $CO_2$ | 758 | 30 | 100% He | 758 | 30 | 50 | 0.45 | 0.43 |
| Derevschikov et al. [16] | 20%CaO80%$Y_2O_3$ | 25% $CO_2$ | 740 | 10 | 100% Ar | 740 | 10 | 120 | 0.06 | 0.10 |
| Zhao et al. [6] | 65%CaO35%$SiO_2$ | 67% $CO_2$ | 600 | 60 | 100% $N_2$ | 700 | 5 | 50 | 0.48 | 0.34 |
| Lu et al. [17] | $n_{Zr}$:$n_{Ca}$=3:10, by FSP [a] | 30% $CO_2$ | 700 | 30 | 100% He | 700 | 30 | 100 | 0.30 | 0.30 |
| | $n_{Zr}$:$n_{Ca}$=3:10, by FSP [a] | 100% $CO_2$ | 850 | 10 | 30% $CO_2$ | 950 | 0 | 23 | 0.25 | 0.23 |
| | $n_{Zr}$:$n_{Ca}$=3:10, by FSP [a] | 30% $CO_2$ | 750 | 10 | 100% He | 750 | 10 | 50 | 0.31 | 0.32 |
| | $n_{Zr}$:$n_{Ca}$=3:10, by wet impregnation | 30% $CO_2$ | 750 | 10 | 100% He | 750 | 10 | 50 | 0.31 | 0.15 |
| Koirala et al. [18] | $n_{Zr}$:$n_{Ca}$=3:10 (41 wt% $CaZrO_3$) [b,c] | 100% $CO_2$ | 700 | 30 | 100% He | 700 | 30 | 100 | 0.34 | 0.33 |
| | $n_{Zr}$:$n_{Ca}$=5:10 (56 wt% $CaZrO_3$) [b,c] | 100% $CO_2$ | 700 | 30 | 100% He | 700 | 30 | 100 | 0.23 | 0.23 |
| | $n_{Zr}$:$n_{Ca}$=5:10 (56 wt% $CaZrO_3$) [b,c] | 100% $CO_2$ | 850 | 10 | 30% $CO_2$ | 950 | 10 | 100 | 0.21 | 0.21 |
| Radfarnia and Iliuta [19] | $n_{Zr}$:$n_{Ca}$=3.03:10 (by surfactant template-ultrasound method) | 100% $CO_2$ | 600 | 30 | 100% Ar | 750 | 30 | 15 | 0.19 | 0.14 |
| Broda and Muller [20] | $n_{Zr}$:$n_{Ca}$=20:80 (36%$ZrO_2$64%CaO) [d] | 20% $CO_2$ | 650 | 20 | 100% $CO_2$ | 900 | 10 | 10 | ~0.33 [e] | 0.21 |
| | $n_{Zr}$:$n_{Ca}$=10:90 (20%$ZrO_2$80%CaO) [d] | 20% $CO_2$ | 650 | 20 | 100% $CO_2$ | 900 | 10 | 10 | >0.49 [f] | 0.31 |
| | $n_{Zr}$:$n_{Ca}$=5:95 (10%$ZrO_2$90%CaO) [d] | 20% $CO_2$ | 650 | 20 | 100% $CO_2$ | 900 | 10 | 10 | >0.57 [f] | 0.36 |

[a] FSP denotes ‘Flame Spray Pyrolysis’;

[b] Prepared by FSP method;

[c] Phase percentage in mass was determined by quantification of powder XRD patterns;

[d] Prepared by sol-gel method: the precursor of CaO was $Ca(OH)_2$ , and gelling time was 2 h;

[e] The initial uptake was calculated by an average decay rate of 0.5% for a 10-cycle experiment;

[f] The initial uptakes were not indicated in either the paper or the supplementary materials but are estimated to be > 0.49 and > 0.57 Net $CO_2$ uptake (g-$CO_2$/g-sorbent) based on the average decay rate > 0.5% for a 10-cycle experiment;

## Experimental

A suspension of $Ca(OH)_2$ was prepared by adding 50 mmol $Ca(OH)_2$ (Alfa Aesar) in 100 ml ethanol dropwise to 100 ml of aqueous ammonium hydroxide solution (pH=11) under continuous stirring. The $ZrO_2$ precursor was prepared by dissolving $ZrO(NO_3)_2 \cdot xH_2O$ (Sigma-Aldrich) in amounts ranging from 2.52, 5.68 and 9.74 mmol in 50 ml in ethanol; this solution was then added dropwise to 50 ml of ammonium hydroxide solution (pH=11). The resulting hydrolyzed zirconyl nitrate sample was added dropwise to the $Ca(OH)_2$ suspension under vigorous stirring. The suspension was aged at room temperature for 3 h and then dried at 70 $^oC$. The dried powders were calcined at 800 $^oC$ in air for 30 min. These samples are labeled 'as-prepared' sorbent powders.

The as-prepared sorbents (3 mg) were subjected to multiple carbonation-decarbonation cycles (up to 30) in a thermogravimetric analyzer (TGA, Mettler Toledo TGA/DSC1 model) under severe and mild conditions to simulate SESR and PCC, respectively. For 'mild' multicycle runs, the samples were purged in 15% $CO_2$ at 650 $^oC$ for carbonation, and in air at 800 $^oC$ for calcination. For 'severe' runs, 100% $CO_2$ was purged throughout each full cycle and carbonation-decarbonation cycling was realized by a temperature swing between 650 $^oC$ and 950 $^oC$. For practical reasons it was not possible to switch between 15 % $CO_2$ during carbonation and 100 % $CO_2$ during calcination using the equipment available; hence it was necessary to alter the carbonation atmosphere for the severe condition. For both mild and severe conditions, heating and cooling rates were 20 $^oC$/min; carbonation dwell times were 15 min, with no dwell period once the maximum calcination temperature was reached; gas flow rates were 50 ml/min under dry conditions.

Powder X-ray diffraction, XRD, was employed to identify the phases present in the as-prepared powders and powders collected after TGA cycles, for 1, 5, 10 and 30 cycles. XRD data were collected using a Bruker D8 diffractometer (Cu-Kα λ=1.5416 Å). The as-prepared powders (~1 g) were loaded in the 25 mm (diameter) well of a polymethylmethacrylate sample holder; for smaller quantities generated by the TGA experiments, the powders (~3 mg) were deposited on a silicon sample holder. It should be noted that there is some additional (Bragg) scattering from the silicon holder visible in the latter patterns. The resulting XRD patterns were analyzed using the X'Pert HighScore Plus software (Version 3.0e). The positions, intensities and shapes of the peaks were measured and matched to known powder diffraction files, using the ICDD PDF4 database (International Centre for Diffraction Data). Rietveld refinements of the diffractograms were performed to quantify the mass fraction of phases present using the X'pert HishScore Plus Software. Details of the methods can be found elsewhere [25, 26].

The microstructure of carbonated and decarbonated sorbents was characterized by scanning electron microscopy, SEM, using a LEO 1530 Gemini field emission gun (FEG-) SEM to scan the surface of the powder samples at 3 keV and a 3.7 mm working distance using an in-lens secondary electron detector. All samples for SEM were sputter coated with a layer of platinum, ~5 nm thick. Transmission electron microscopy, TEM, was employed to gain insights into the detailed structure of the sorbent powders by: selected area electron diffraction (SAED); atomic lattice imaging; energy dispersive X-ray (EDX) spectroscopy and elemental mapping. For this purpose a Philips CM200 FEG-TEM was operated at 197 keV and fitted with a Gatan Imaging Filter (GIF 200) and an Oxford Instruments 80 $mm^2$ Xmax SDD EDX spectrometer running the AZTEC processing software. Samples were prepared by dispersing sorbents in ethanol and drop-casting onto holey carbon TEM support films (Agar Scientific Ltd).

## Results and Discussion

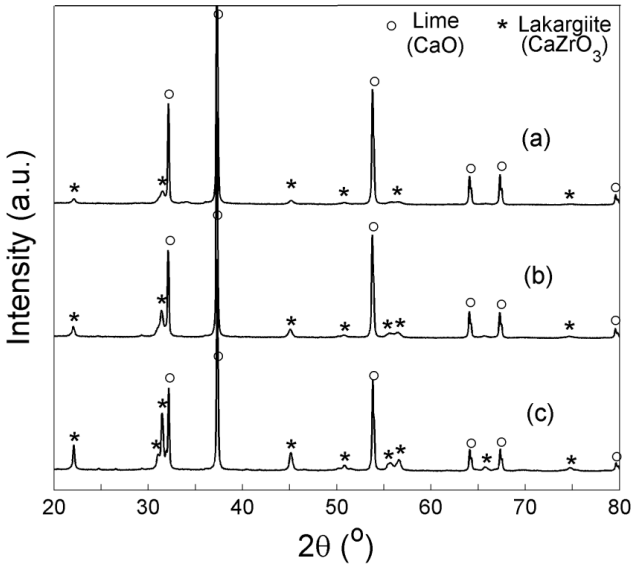


**Figure 1.** XRD patterns for the as-prepared sorbents (freshly calcined at 800 °C), (a) Sample 1, 10(wt%)$CaZrO_3$:90(wt%)CaO, (b) Sample 2, 18$CaZrO_3$:82CaO, and (c) Sample 3 30$CaZrO_3$:70CaO.

The as-prepared sorbent powders contained a mixture of CaO (cubic) and $CaZrO_3$ (orthorhombic), as identified by powder XRD [27] (**Figure 1**). Rietveld refinement of the XRD data for as-prepared powders and for powders after multiple TGA carbonation/decarbonation cycles gave residual ($R_P$) and weighted residual ($R_{WP}$) Rietveld parameters <10% (Figure S1, Table S1), indicating that the model provided a reliable indication of phase proportions (accurate to ± 1 wt%) [22]. The estimated weight fraction (%) of $CaZrO_3$ in the three as-prepared sorbents were as follows: Sample 1, 10$CaZrO_3$:90CaO; Sample 2, 18$CaZrO_3$:82CaO; Sample 3, 30$CaZrO_3$:70CaO. After 10 or 30 TGA cycles, each terminating with calcination, the equivalent

CaO (CaO + $CaCO_3$) to $CaZrO_3$ mass ratios were the same as for the as-prepared powders, indicating the initial calcination step had achieved complete reaction.

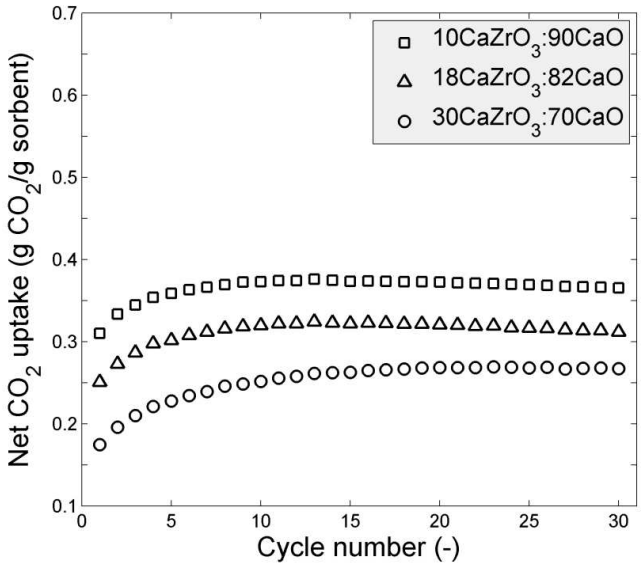


**Figure 2.** Cyclic $CO_2$-capture performance under the 'mild' conditions (carbonation: 15% $CO_2$, 650 $^oC$, 15min; calcination: air, 800 $^oC$, no dwell time)

**Table 2.** Net $CO_2$ uptakes and carbonation percentages for cycle 1, 10 and 30 under 'mild' conditions (carbonation: 15% $CO_2$, 650 $^oC$, 15min; calcination: air, 800 $^oC$, no dwell time)

| | Carbonation | | | Calcination | | | Net $CO_2$ uptake (g-$CO_2$/g-sorbent) | | | Carbonation (%) | | |
|---|---|---|---|---|---|---|---|---|---|---|---|---|
| | Gas | *T* ($^oC$) | *t* (min) | Gas | *T* ($^oC$) | *t* (min) | 1st | 10th | 30th | 1st | 10th | 30th |
| 10$CaZrO_3$:90CaO | | | | | | | 0.310 | 0.373 | 0.365 | 43.8 | 52.7 | 51.6 |
| 18$CaZrO_3$:82CaO | 15% $CO_2$ | 650 | 15 | air | 800 | 0 | 0.251 | 0.320 | 0.312 | 39.0 | 49.7 | 48.4 |
| 30$CaZrO_3$:70CaO | | | | | | | 0.175 | 0.251 | 0.267 | 31.8 | 45.6 | 48.5 |

The net $CO_2$ uptakes, expressed as g-$CO_2$/g-total sorbent mixture, using the three as-prepared sorbent compositions under 'mild' conditions are shown in **Figure 2** (15% $CO_2$ at 650 $^oC$ for

carbonation, and in air at 800 $^{o}$C); the specific $CO_2$ uptakes in cycle 1, 10 and 30 are listed in **Table 2** accompanied with molar carbonation percentages of the CaO component, calculated according to Equation 1:

$$Carbonation\ (\%) = 100\% \times \frac{\text{Net mass of } CO_2 \text{ uptake (g } CO_2)/44}{\text{CaO initial mass (g CaO)}/56} \qquad \text{Eq. (1)}$$

Each of the sorbent blends showed an increase in uptake capacity in the first ~10 cycles, with little further variation over the full 30 cycles tested. For Sample 1, the $CO_2$ uptake increased: from 0.310 to 0.373 g-$CO_2$/g-sorbent between cycle 1 and cycle 10; and for Sample 2 from 0.251 to 0.320 g-$CO_2$/g-sorbent. After cycle 10 a near-stable $CO_2$ uptake was demonstrated over the 30 cycles tested, retaining these capacities at cycle 30. For Sample 3, a continuous increase was observed after cycle 10 and the $CO_2$ uptake reached 0.267 g-$CO_2$/g-sorbent. Sample 3 showed the lowest initial molar carbonation, 31.8%, of the three sorbents. However, after cycle 30, 48.5% of the CaO in Sample 3 was carbonated, in line with Sample 1 and 2 (Table 2).

An initial increase in capacity has been observed for other CaO blends and is often referred to as 'self-reactivation' [28]. To understand this here, we chose to investigate the detailed microstructure of Sample 3 because of it exhibits the most significant increase in molar carbonation with cycles. The reasons behind this increase were revealed by SEM which showed a densely packed microstructure with little porosity in the as-prepared powder yet at cycle 10 the powder matrix was more porous, containing <100 nm pores within a matrix of <200 nm CaO particles (**Figure 3**). This development of a more porous matrix in the first 10 carbonation-calcination cycles accounts for the observed rise in $CO_2$ capacity; progressive change to this microstructure in the earlier cycles would give rise to the gradual increase in $CO_2$ uptake that is observed.

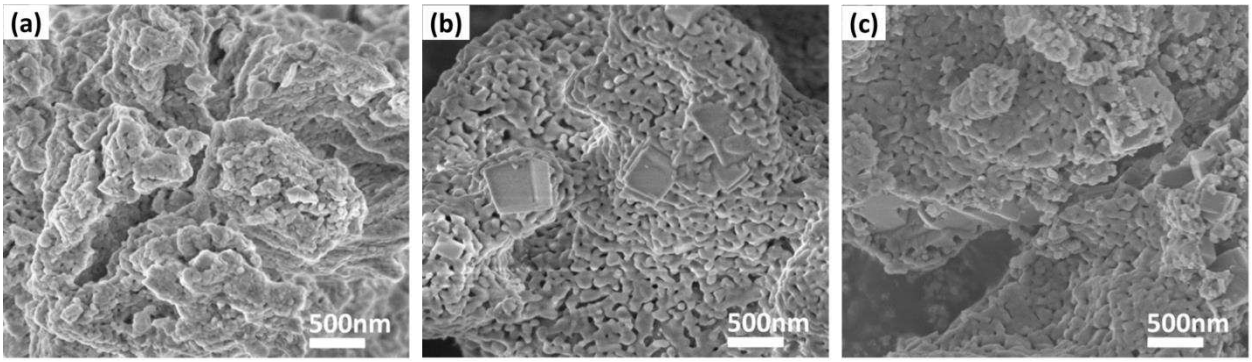


**Figure 3.** SEM images of porosity development within Sample 3, the $30CaZrO_3$:70CaO sorbent after the 'mild' TGA cycles ending on calcination (carbonation: 15% $CO_2$, 650 $^oC$, 15min; calcination: air, 800 $^oC$, no dwell time). (a) Fresh form, (b) after 10 cycles, (c) after 30 cycles. The cuboid particles evident in b and c are identified as $CaZrO_3$ micro-particles by TEM (Figure 8).

A single TGA cycle for Sample 3, the $30CaZrO_3$70CaO sorbent under the 'mild' conditions (carbonation: 15% $CO_2$, 650 $^oC$, 15min; calcination: air, 800 $^oC$, no dwell time) for each of cycles 1, 5, 10 and 30 are shown in **Figure 4**. The most notable feature is the change in the TGA carbonation profile between cycle 1 and cycle 5. No significant linear region is observed in cycle 1: the curvature to the profile over the full 15 min treatment and a $t^n$ rate dependence over the total 18 wt% increase, indicates the carbonation kinetics are dominated by solid state diffusion of $CO_2$ through a $CaCO_3$ layer [29, 30]. By cycle 5, ~18 wt% of a total of 25 wt% mass gain in the carbonation step is associated with rapid linear kinetics, suggesting a surface reaction between $CO_2$ and exposed CaO particles [29, 30]. Cycles 10 and 30 are very similar to cycle 5. The interpretation of these TGA profiles complements the microstructural observations by SEM (Figure 3): the carbonation in cycle 1 involves a densely packed powder and so only a very minor proportion of the total carbonation reaction occurs by gas-solid reaction (linear kinetics)

and the carbonation reaction is dominated by solid state diffusion. For later cycles the series of carbonation-decarbonation, volume changing reactions has created porosity in the CaO powder (Figure 3). (Most of this porosity will be created when the densified $CaCO_3$ particles decompose during calcination (**Figure 5**). Hence a higher specific surface area becomes available for gas-solid chemical reactions, and a higher proportion of the carbonation reaction rate is controlled by the linear chemical kinetics of the surface reaction of $CO_2$ with CaO.

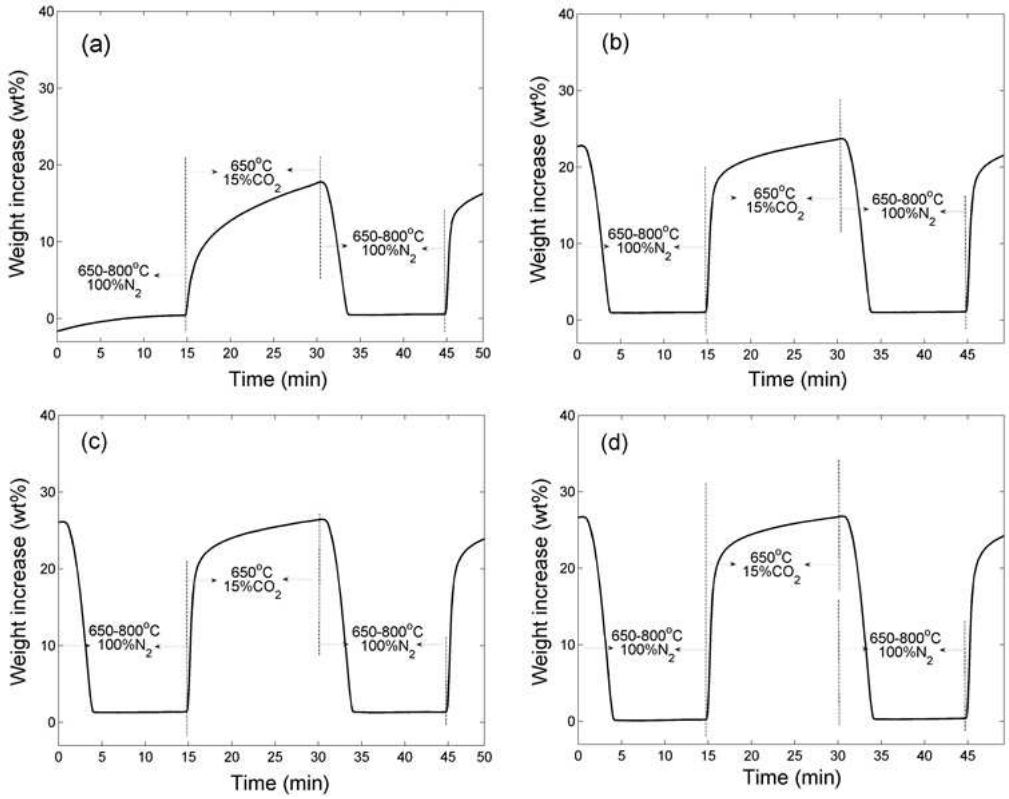


**Figure 4.** TGA weight profiles with time for Sample 3, the $30CaZrO_3$:70CaO sorbent under the 'mild' conditions (carbonation: 15% $CO_2$, 650 $^oC$, 15min; calcination: air, 800 $^oC$, no dwell time) for: (a) cycle 1, (b) cycle 5, (c) cycle 10 and (d) cycle 30. Note the initial baseline drift of the TGA (first cycle Figure 4a) stabilizes after one complete cycle.

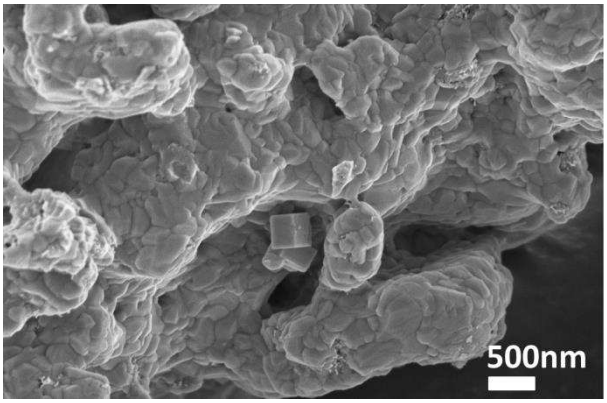


**Figure 5.** SEM image of the densified microstructure of Sample 3, the 30$CaZrO_3$70CaO sorbent after 10 'mild' TGA cycles (carbonation: 15% $CO_2$, 650 $^oC$, 15min; calcination: air, 800 $^oC$, no dwell time) when ending on carbonation

The multicycle results for severe calcination conditions, 950°C in 100 % $CO_2$, in which carbonation also occurred in 100 % $CO_2$, are shown in **Figure 6**. As expected, carbonation in 100% $CO_2$ led to a greater molar conversion than in 15 % $CO_2$. The Cycle 1 $CO_2$ uptakes were 0.46, 0.43 and 0.36, g-$CO_2$/g-sorbent, for Samples 1, 2 and 3 respectively. Sample 3 with its increased $CaZrO_3$ content of 30 (wt%) was studied because of its better durability under severe conditions than for Samples 1 and 2 i.e. it shows the lowest decline in capture capacity (Figure 6) and the greatest percentage of carbonation (Table 3). A decline in capture capacity over prolonged cycling occurred for these severe calcination conditions, this is in contrast to the very stable performance in prolonged multicycle operation for mild calcination at 800 °C. For example, the uptake decayed from 0.36 g-$CO_2$/g-sorbent at cycle 1 to 0.31 g-$CO_2$/g-sorbent by cycle 30 for Sample 3, representing a decline of <14% of the initial value (**Table 3**). Examination of SEM micrographs indicated an increased degree of inter-particle necking with increasing number of calcination cycles, and a slight increase in particle size (relative to the mild

conditions), **Figure 7**. The resulting reduction in solid-gas interfacial area, cycle-on-cycle, gives rise to the decrease in uptake capacity.

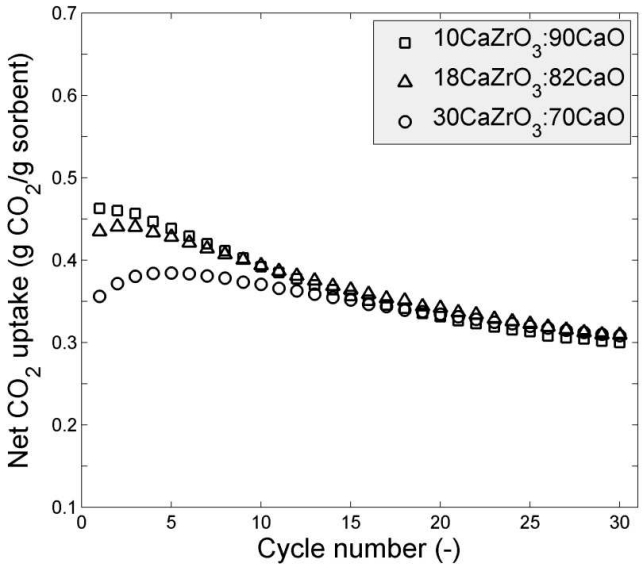


**Figure 6.** Cyclic $CO_2$-capture performance under the 'severe' conditions (carbonation: 100% $CO_2$, 650 $^oC$, 15min; calcination: 100% $CO_2$, 950 $^oC$, no dwell time).

**Table 3** Net $CO_2$ uptakes and carbonation percentages for cycle 1, 10 and 30 under the 'severe' conditions (carbonation: 100% $CO_2$, 650 $^oC$, 15min; calcination: 100% $CO_2$, 950 $^oC$, no dwell time)

| | Carbonation | | | Calcination | | | Net $CO_2$ uptake (g-$CO_2$/g-sorbent) | | | Carbonation (%) | | |
|---|---|---|---|---|---|---|---|---|---|---|---|---|
| | Gas | $T$ ($^oC$) | $t$ (min) | Gas | $T$ ($^oC$) | $t$ (min) | 1st | 10th | 30th | 1st | 10th | 30th |
| $10CaZrO_3$:90CaO | | | | | | | 0.46 | 0.39 | 0.30 | 65.4 | 55.4 | 42.4 |
| $18CaZrO_3$:82CaO | 100% $CO_2$ | 650 | 15 | 100% $CO_2$ | 950 | 0 | 0.43 | 0.39 | 0.31 | 69.1 | 62.6 | 49.2 |
| $30CaZrO_3$:70CaO | | | | | | | 0.36 | 0.37 | 0.31 | 64.7 | 67.4 | 56.1 |

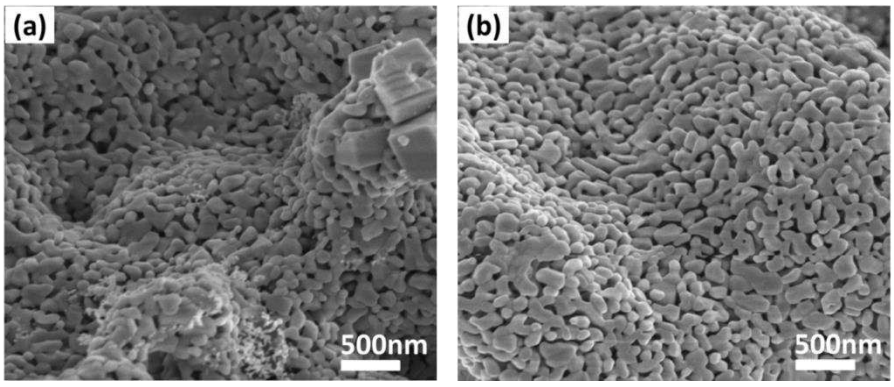


**Figure 7.** SEM images of the particle growth and necking for Sample 3, the 30$CaZrO_3$:70CaO sorbent after the 'severe' TGA cycles ending on calcination (carbonation: 15% $CO_2$, 650 $^oC$, 15min; calcination: air, 800 $^oC$, no dwell time). (a) after 10 cycles, (b) after 30 cycles

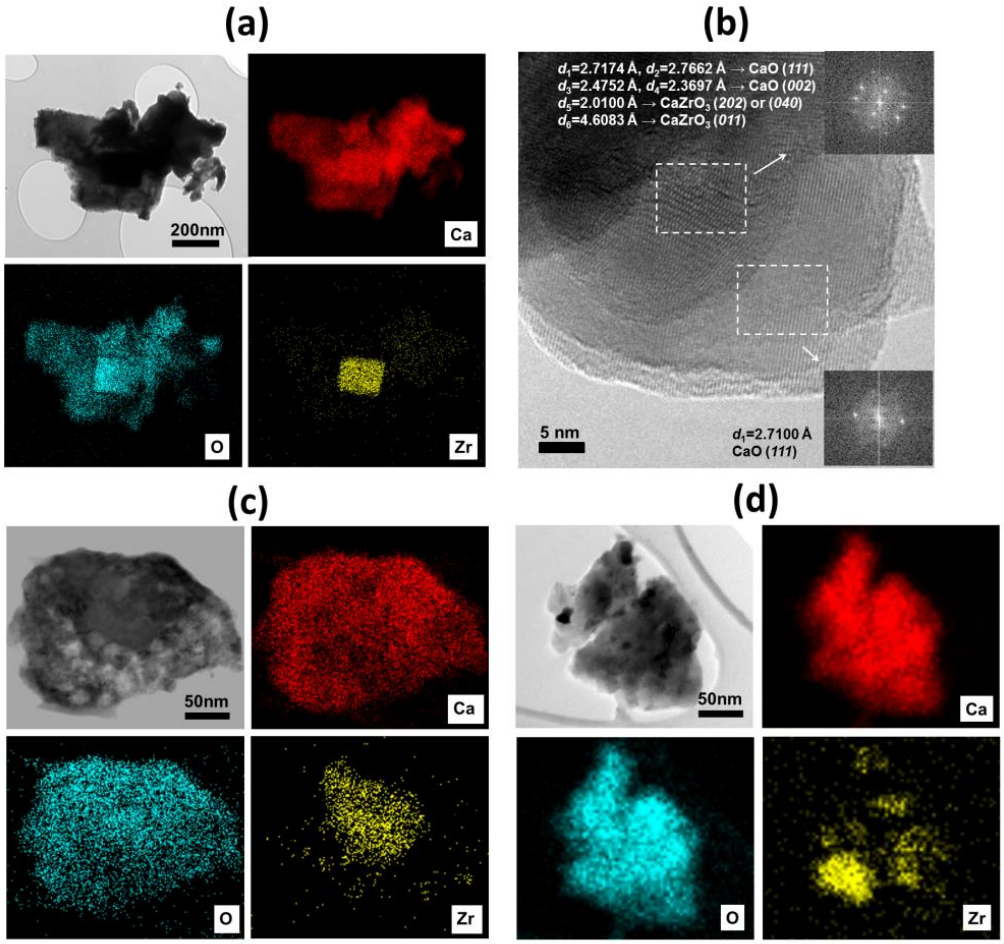

**Figure 8.** TEM analysis of Sample 3, the 30$CaZrO_3$70CaO sorbent: (a) TEM bright field image and associated elemental X-ray maps for the freshly calcined sorbent, (b) atomic lattice image and inset Fourier transforms indexed to CaO or $CaZrO_3$ phases for the freshly calcined sorbent, (c) TEM bright field image and associated elemental X-ray maps for the spent sorbent from cycle 10 under the 'mild' conditions ending on calcination, and (d) TEM bright field image and associated elemental X-ray maps for the spent sorbent from cycle 30 under the 'mild' conditions ending with calcination.

Examples of TEM analysis of as-prepared powders and powders after multiple TGA mild cycles are shown in **Figure 8**. Elemental Zr mapping of a group of particles in an as- prepared powder (Figure 8a), highlights a Zr rich region ~150 nm in size that corresponds to one of the $CaZrO_3$ cuboid particles first identified by SEM (Figure 3). Much smaller Zr containing regions were also identified, dispersed throughout the matrix: selected area electron diffraction (not shown) and lattice imaging revealed these Zr signals were due to nanoscale particles of $CaZrO_3$, 20-80 nm in size, distributed within the ≤ 200 nm CaO particle matrix, (Figure 8b). Particles after 10 and 30 cycles (ending with calcination) are shown in Figures 8c and 8d respectively. The EDX elemental mapping implies that some intra-particle segregation of $CaZrO_3$ nanoparticles may have occurred on repeat cycling, but this did not affect durability in the mild cycles (Figure 2). It is assumed that the near-stable $CO_2$ capture durability from the $CaZrO_3$/CaO powders is due principally to these $CaZrO_3$ nanoparticles acting as spacers to suppress densification and loss of micro- or meso-porosity during repeated calcinations. Whilst it is possible that a very limited range of solid solution (< 1%) forms between CaO and $ZrO_2$ [31] there was no evidence of this from XRD lattice spacing measurements.

Powders from flame spray pyrolysis (FSP) were reported to have optimal durability at $n_{Zr}$: $n_{Ca}$ = 3:10 [17], later revised to the more dilute blend $n_{Zr}$:$n_{Ca}$ = 5:10 [18], containing 56% $CaZrO_3$. This is almost double the amount of $CaZrO_3$ in Sample 3 of the present work, yet the initial molar conversion ratios are similar, probably because of the smaller CaO particle size from FSP and the higher temperatures and $CO_2$ partial pressures used for the carbonation step in the FSP trials. Both powder types display comparable durability under mild conditions, but the FSP show slightly better stability at higher temperatures probably in part due to the higher $CaZrO_3$ content. The overall performance of the present powders is superior in terms of initial uptake capacity and multicycle durability when compared to several other Zr modified CaO powders produced by wet chemical routes [17, 19]. The new powders presented here show negligible decay in $CO_2$ capacity within the 30 cycles tested under decarbonation at 800 °C: merely 2% decrease was observed in net $CO_2$ uptake from cycle 10 to cycle 30, and near-flat molar conversion ratios of > 50% were recorded for Sample 1, the 10$CaZrO_3$:90CaO sorbent (Table 2). A co-precipitation method, from Zr and Ca salt solutions, produced powders which showed a drop in conversion ratio from > 60% to ~40% after 10 cycles falling further to ~35 % after 30 mild calcination cycles at 750 °C [17]. Another wet chemical method, based on a surfactant template ultrasound chemical route showed an initial uptake of only 0.19 g-$CO_2$/ g-sorbent in cycle 1 decaying to 0.14 g-$CO_2$/ g-sorbent in cycle 15, for calcination temperatures 750 °C [19], compared to an uptake stabilizing at 0.37 g-$CO_2$/g-sorbent in this work. A sorbent produced by a sol-gel synthesis route with $n_{Zr}$:$n_{Ca}$ = 20:80, containing 36 wt% $ZrO_2$ (equivalent to 52 wt% $CaZrO_3$: 48 wt% CaO assuming full conversion) exhibited an initial capacity of 0.33 g-$CO_2$/g-sorbent decreasing to 0.21 g-$CO_2$/g-sorbent at cycle 10. This represents a relative decline of 36% in 10 cycles (carbonation in 20% $CO_2$ at 650 $^oC$ for 20 min and calcination in 100% $CO_2$ at 900 $^oC$ for

10 min) [20]. The uptake of the present 30wt%$CaZrO_3$:70wt%CaO sorbent (carbonation in 100 % $CO_2$ at 650 °C and calcination in 100 % $CO_2$ at 950 °C) increased slightly from 0.36 (initial) to 0.39 g-$CO_2$/g-sorbent (cycle 4) and then steadily decayed to 0.37 g-$CO_2$/g-sorbent at cycle 10, reaching 0.31 g-$CO_2$/g-sorbent at cycle 30 representing a decreased of ~14% over 30 cycles. It should be noted that the wet chemical method described in this work is relatively simple in comparison to other methods such as FSP, ultrasound-assisted surfactant template synthesis and sol-gel synthesis which will have a favorable impact on processing costs.

In terms of comparisons between the present $CaZrO_3$:CaO powders and other CaO based sorbent compositions, an optimum 25wt%$Ca_{12}Al_{14}O_{33}$:75wt%CaO blend maintained an uptake of 0.45 g-$CO_2$/g-sorbent for up to 13 'mild' cycles for calcination at 850 °C in $N_2$ for 10 min, Table 1 [9]. Martavaltzi and Lemonidou [10] reported similar performance for this type of sorbent. When calcination temperatures are raised to 950 °C, which are more realistic for PCC applications, capacity decayed from 0.4 to 0.33 g-$CO_2$/g-sorbent after 13 cycles. This compares to a change from 0.36 g -$CO_2$/g-sorbent to 0.31 g-$CO_2$/g-sorbent after 30 cycles for 30$CaZrO_3$:70CaO (Sample 3); this capacity at 30 cycles is much higher than the data extrapolated to 30 cycles in Li et al. [9] Koirala et al. [11] synthesized a $Ca_{12}Al_{14}O_{33}$/CaO sorbent ($n_{Al}$:$n_{Ca}$=3:10) by a single nozzle flame spray pyrolysis (FSP) method and reported near-stable $CO_2$ uptake to the 100$^{th}$ cycle of ~ 0.40 g $CO_2$/g sorbent for mild calcination at 700 °C for 10 min, but this decreased to 0.25 g-$CO_2$/g-sorbent for calcination at 950 °C for 10 min in 30 % $CO_2$. Broda and Muller have prepared a $Ca_{12}Al_{14}O_{33}$:CaO sorbent using a sophisticated organic template synthesis method in which particle sizes were ~170 nm [12]. The resorcinol/formaldehyde and aqueous Ca-Al precursors underwent a 3-day gelation followed by calcination in an inert atmosphere, which formed nano-sized carbonaceous spheres coated with Ca-Al species. Hollow

spherical calcium oxide/calcium aluminate particles were obtained after removing the carbon templates. The improved microstructure enabled a near-stable performance for up to 30 cycles for calcination at 750 °C in $N_2$ with a capacity of ~0.55 g-$CO_2$/g-sorbent. However, the complicated production of the sorbent can hardly be realized at larger scales.

Yu and Chen [13] modified a $Ca_{12}Al_{14}O_{33}$ stabilized CaO sorbent powder ($n_{Al}$:$n_{Ca}$=3:10) using an additional $TiO_2$ binder. A drop from 0.40 to 0.36 g-$CO_2$/g-sorbent ($n_{Al}$:$n_{Ca}$=3:10) was reported for a long carbonation time, 60 min, and calcination at 750 °C for 30 min in $N_2$. Such long reaction times are not feasible for industrial operations.

Wu and Zhu [14] used 17 wt% $CaTiO_3$ as a spacer to maintain a stable $CO_2$ uptake at 0.23 g-$CO_2$/g-sorbent over 10 mild reaction cycles for calcination at 750 C for 10 min in $N_2$. Li et al. [15] used 42 wt% MgO in CaO and attained stable uptake of ~0.43 g-$CO_2$/g-sorbent over 50 cycles for calcination temperatures of 758 $^oC$ (and carbonation times of 30 min). Derevschikov et al. [16] added 80 wt% $Y_2O_3$ to CaO powders to obtain a very stable sorbent but with a net $CO_2$ uptake capacity of only ~0.1 g-$CO_2$/g-sorbent (calcination 740 °C for 10 min in Argon. Zhao et al. [6] used 33 mol% $SiO_2$ as a stabilizer to produce a performance that dropped from 0.48 to 0.34 g-$CO_2$/g-sorbent over 50 mild reaction cycles, 700 $^oC$ for $\leq$ 60 min.

Overall, the present powders compare favourably in terms of multicycle sorbent performance to previously reported CaO based materials. The key to further improving the high temperature durability of $CaZrO_3$/CaO lies in refining solution synthesis conditions to reduce the proportion of cuboid $CaZrO_3$ microparticles and maximize the proportion of $CaZrO_3$ nanoparticles within the CaO matrix.

## Conclusions

Powder sorbents of CaO modified with $CaZrO_3$ were prepared in three different component ratios as identified by Rietveld refinement of X-ray diffraction data: 10 wt%, 18wt % and 30 wt% $CaZrO_3$. The $CO_2$ capture performance was evaluated over 30 carbonation/decarbonation cycles for two sets of conditions. The overall performance of the powders compare favourably to other Zr modified CaO powders produced by different wet chemical routes. Near-stable multicycle $CO_2$ uptake was demonstrated for calcination at 800 °C in air after prolonged thermal cycling (30 cycles tested). For example, a $CO_2$ uptake capacity of 0.373 g-$CO_2$/g-sorbent (for cycle 10) decreasing very slightly to 0.365 g-$CO_2$/g-sorbent (for cycle 30) was demonstrated for a 10(wt.)%$CaZrO_3$:90%CaO powder blend. These powders may prove to be useful in sorption enhanced steam reforming applications. Under severe calcination conditions, 950 °C in 100% $CO_2$ (calcination 650 °C in 100 % $CO_2$, 15 min), the most durable composition, 30%$CaZrO_3$:70%CaO demonstrated an uptake of 0.36 g-$CO_2$/g-sorbent in cycle 1 decreasing to 0.31 by cycle 30.

CORRESPONDING AUTHOR

* Phone: +44 113 343 8592, email: simon.ming.zhao@gmail.com.

ACKNOWLEDGMENT

The authors acknowledge the financial support of the EPSRC for grant EP/J014702/1.

SUPPORTING INFORMATION

The quality of Rietveld Refinement for the as-prepared and cycled sorbent powders is shown in Figure S1 and Table S2. This information is available free of charge via the Internet at http://pubs.acs.org/.

REFERENCES


1. Anthony, E. J.; Bulewicz, E. M.; Jia, L. *Prog. Energy Combust. Sci.* **2007,** 33, (2), 171-210.

2. Abanades, J. C.; Anthony, E. J.; Wang, J.; Oakey, J. E. *Environ. Sci. Technol.* **2005,** 39, (8), 2861-2866.

3. Dou, B.; Dupont, V.; Rickett, G.; Blakeman, N.; Williams, P. T.; Chen, H.; Ding, Y.; Ghadiri, M. *Bioresour. Technol.* **2009,** 100, (14), 3540-3547.

4. Pimenidou, P.; Rickett, G.; Dupont, V.; Twigg, M. V. *Bioresour. Technol.* **2010,** 101, (23), 9279-9286.

5. Ramkumar, S.; Phalak, N.; Fan, L.-S. *Ind. Eng. Chem. Res.* **2011,** 51, (3), 1186-1192.

6. Zhao, M.; Yang, X.; Church, T. L.; Harris, A. T. *Environ. Sci. Technol.* **2012,** 46, (5), 2976-83.

7. MacKenzie, A.; Granatstein, D. L.; Anthony, E. J.; Abanades, J. C. *Energy Fuels* **2007,** 21, (2), 920-926.

8. Manovic, V.; Charland, J. P.; Blamey, J.; Fennell, P. S.; Lu, D. Y.; Anthony, E. J. *Fuel* **2009,** 88, (10), 1893-1900.

9. Li, Z.-s.; Cai, N.-s.; Huang, Y.-y.; Han, H.-j. *Energy Fuels* **2005,** 19, (4), 1447-1452.

10. Martavaltzi, C. S.; Lemonidou, A. A. *Ind. Eng. Chem. Res.* **2008,** 47, (23), 9537-9543.

11. Koirala, R.; Reddy, G. K.; Smirniotis, P. G. *Energy Fuels* **2012,** 26, (5), 3103-3109.

12. Broda, M.; Müller, C. R. *Adv. Mater.* **2012,** 24, (22), 3059-3064.

13. Yu, C.-T.; Chen, W.-C. *Powder Technol.* **2013,** 239, (0), 492-498.

14. Wu, S. F.; Zhu, Y. Q. *Ind. Eng. Chem. Res.* **2010,** 49, (6), 2701-2706.

15. Li, L.; King, D. L.; Nie, Z.; Howard, C. *Ind. Eng. Chem. Res.* **2009,** 48, (23), 10604-10613.

16. Derevschikov, V. S.; Lysikov, A. I.; Okunev, A. G. *Ind. Eng. Chem. Res.* **2011,** 50, (22), 12741-12749.

17. Lu, H.; Khan, A.; Pratsinis, S. E.; Smirniotis, P. G. *Energy Fuels* **2008,** 23, (2), 1093-1100.

18. Koirala, R.; Gunugunuri, K. R.; Pratsinis, S. E.; Smirniotis, P. G. *J. Phy. Chem. C* **2011,** 115, (50), 24804-24812.

19. Radfarnia, H. R.; Iliuta, M. C. *Ind. Eng. Chem. Res.* **2012,** 51, (31), 10390-10398.

20. Broda, M.; Müller, C. R. *Fuel* **2013**, http://dx.doi.org/10.1016/j.fuel.2013.08.004.

21. Vasconcelos, C. New Challenges in the Sintering of HA/$ZrO_2$ Composites. In *Sintering of Ceramics - New Emerging Techniques*, Lakshmanan, A., Ed. InTech: 2012.

22. Molinder, R.; Comyn, T. P.; Hondow, N.; Parker, J. E.; Dupont, V. *Energy Environ. Sci.* **2012,** 5, (10), 8958-8969.

23. Donat, F.; Florin, N. H.; Anthony, E. J.; Fennell, P. S. *Environ. Sci. Technol.* **2011,** 46, (2), 1262-1269.

24. Blamey, J.; Lu, D. Y.; Fennell, P. S.; Anthony, E. J. *Ind. Eng. Chem. Res.* **2011,** 50, (17), 10329-10334.

25. Meethong, N.; Huang, H. Y. S.; Speakman, S. A.; Carter, W. C.; Chiang, Y. M. *Adv. Funct. Mater*. **2007**, 17, (7), 1115–1123.

26. Wang, Z.; Comyn, T. P.; Ghadiri, M.; Kale, G. M. *J. Mater. Chem.* **2011**, 21, 16494–1649.

27. CaO: ICDD-PDF-04-011-8430 (Lime, syn); $CaZrO_3$: ICDD-PDF-04-010-6396 (Lakargiite, syn). In.

28. Manovic, V.; Anthony, E. J. *Int. J. Environ. Res. Public Health* **2010,** 7, (8), 3129-3140.

29. Florin, N. H.; Harris, A. T. *Energy Fuels* **2008,** 22, (4), 2734-2742.

30. Yang, Z.; Zhao, M.; Florin, N. H.; Harris, A. T. *Ind. Eng. Chem. Res.* **2009,** 48, (24), 10765-10770.

31. Du, Y.; Jin, Z.; Huang, P. *J. Am. Ceram. Soc.* **1992,** 75, (11), 3040-3048.